PHYSICAL REVIEW D **90,** 024071 (2014)

Distinguishing black holes and wormholes with orbiting hot spots

Zilong Li and Cosimo Bambi*

Center for Field Theory and Particle Physics & Department of Physics, Fudan University, 200433 Shanghai, China

(Received 9 May 2014; published 25 July 2014)

The supermassive black hole candidates at the center of every normal galaxy might be wormholes created in the early Universe and connecting either two different regions of our Universe or two different universes in a multiverse model. Indeed, the origin of these supermassive objects is not well understood; topological nontrivial structures like wormholes are allowed both in general relativity and in alternative theories of gravity, and current observations cannot rule out such a possibility. In a few years, the VLTI instrument GRAVITY will have the capability to image blobs of plasma orbiting near the innermost stable circular orbit of SgrA*, the supermassive black hole candidate in the Milky Way. The secondary image of a hot spot orbiting around a wormhole is substantially different from that of a hot spot around a black hole, because the photon capture sphere of the wormhole is much smaller. The radius of the photon capture sphere is independent of the hot spot model, and therefore its possible detection, which is observationally challenging but not out of reach, can unambiguously test if the center of our Galaxy harbors a wormhole rather than a black hole.

DOI: 10.1103/PhysRevD.90.024071 PACS numbers: 04.20.-q, 04.70.-s, 98.35.Jk

I. INTRODUCTION

The Einstein equations are local equations relating the geometry of the spacetime to its matter content. There is no information about the spacetime topology. Even if it is far from our common sense, we cannot exclude that our Universe has a nontrivial topology or that it contains topologically nontrivial structures. In this spirit, there is a rich literature on wormholes (WHs)—that is, shortcuts connecting two different regions of our Universe or two different universes in multiverse theories [1]. WH spacetimes are allowed even in alternative theories of gravity. Since they require a change of topology, WHs may not be created in the Universe today, but a number of mechanisms may have worked in the early Universe [2]. Primordial WHs may have survived till today and live somewhere in the Universe. In particular, they have been proposed as candidates for the supermassive objects that are seen at the center of every normal galaxy [3]. These objects are usually supposed to be Kerr black holes (BHs) with masses $M \sim 10^5$–$10^9 M_\odot$, but their actual nature is not known.

In the case of the center of our Galaxy, the central supermassive object has a mass $M \approx 4 \times 10^6 M_\odot$ [4]. An upper bound on its radius can be inferred from the closest distance approached by the orbiting stars. Current data put this bound at about 45 AU, which corresponds to ~600 Schwarzschild radii [5]. Such estimates of the mass and radius can exclude the possibility that the central object is actually a cluster of neutron stars, because the cluster lifetime would only be $\sim 10^5$ yrs, which is much shorter than the age of this system [5,6]. The nonobservations of thermal radiation emitted by the possible surface of this object may also be interpreted as an indication for the presence of an event/apparent horizon [7]. This body of evidence strongly supports the conclusion that the supermassive object at the center of the Galaxy is a supermassive BH. Such a conclusion is naturally extended to all the supermassive objects in galactic nuclei. However, there is no real indication that the spacetime geometry around these bodies is described by the Kerr solution [8] (for a review, see e.g., Ref. [9]). There are also open questions about their formation and growth. Any competitive model must be able to explain how they were able to become so heavy in a very short time, as we know of BH candidates with mass $M \sim 10^9 M_\odot$ at redshift $z \gtrsim 6$, i.e., just about 100 million years after the Big Bang [10]. While there are potentially many possibilities, we do not know which one is correct [11]. Scenarios in which the seeds of these supermassive objects are a relic of the very early Universe are also possible [12], and in this context there is room for WHs too [2].

While of exotic nature, at least some kinds of primordial WHs can be viable candidates to explain the supermassive objects at the centers of galaxies. These objects have no solid surface, and therefore they may mimic the presence of an event horizon. They would have been produced in the early Universe and grown during inflation, which could explain their presence even at very high redshift. They have a positive effective mass, and therefore a WH can swallow material from an accretion disk, and two WHs can merge when their host galaxies merge. All these processes make the effective mass of the WH increase, as the new material is trapped in the WH throat and, even if the latter is long, there is no spread, or only a small spread, of the

*Corresponding author.
bambi@fudan.edu.cn

gravitational strength lines. WHs can behave in the same way as BHs, even if the physics inside the WH throat can be very different from that inside the BH event horizon. For these reasons, WHs can be as good as BHs to explain the observed correlations between the supermassive BH candidates and the host galaxies [13]. Another important issue is the formation of relativistic jets, which are commonly observed from BH candidates. At present, we do not know the actual mechanism responsible for the formation of these jets, and there are several models in the literature. If the jets are powered by the rotational energy of the compact object, the Blandford-Znajek process [14], the WHs discussed in this paper cannot have a jet, as they are nonrotating. Fast-rotating WHs seem to be already ruled out by current observations [15]. However, all the other mechanisms in which jets are powered by the rotational energy of the disk or by the mass accretion rate (see e.g., Ref. [16]) can perfectly work around a WH without any modification. Current observations cannot yet provide an answer, and the topic is very controversial [17].

On the basis of these considerations, it seems that WHs can be serious candidates to explain the supermassive objects in galactic nuclei. It is therefore a natural question to wonder whether astrophysical observations can distinguish Kerr BHs and WHs and thus test the WH scenario. Despite the clear difference between BHs and WHs, current observations cannot rule out the possibility that the supermassive objects in galactic nuclei are WHs instead of BHs. In Ref. [15], one of us considered a particular family of traversable WHs and studied the possibility of distinguishing BHs and WHs from the analysis of the iron Kα line. The latter is a very narrow emission line at about 6.4 keV, but the one observed in the spectra of supermassive BH candidates is broad and skewed, as a result of special and general relativistic effects. In Ref. [15], it was found that the iron line profile produced in the accretion disk of a nonrotating WH looks like the one emitted from a disk around a Kerr BH with spin parameter $a_* \approx 0.8$. More in general, WHs with spin parameter $a_* \lesssim 0.02$ may be interpreted as Kerr BHs with a spin parameter in the range $a_* \approx 0.8$–1.0, while WHs with spin parameter larger than 0.02 have substantially different iron lines and can be ruled out because they are inconsistent with observations. The constraints found in Ref. [15] and the fact that accretion and merger processes should spin the WH up may have two possible explanations: (i) rotating WHs are unstable, and therefore, even if a WH gets angular momentum, the latter is quickly lost, for instance via the emission of gravitational waves; or (ii) fast-rotating WHs different from the ones considered in Ref. [15] are consistent with current observations; unlike Kerr BHs in general relativity, here there is no uniqueness theorem, so the conclusions of Ref. [15] cannot be definitive.

The possibility of observationally testing the idea that the supermassive objects in galactic nuclei are WHs was further discussed in Ref. [18], where it was pointed out that it would be relatively easy to figure out if SgrA* is a WH or a BH from the observation of its "shadow." The latter is a dark area over a brighter background seen by a distant observer if the compact object is surrounded by optically thin emitting material and corresponds to the apparent photon capture sphere [19]. While the exact shape and size of the shadow of Kerr and non-Kerr BHs is extremely similar [20], and at present it is not completely clear if its future detection can constrain possible deviations from the Kerr solution, the shadow of a WH is much smaller than that of a BH, and it is therefore distinguishable even without an accurate detection and with all the systematic effects that significantly tangle the job [18].

In the present paper, we further extend the study of Refs. [15,18], and we investigate the possibility of testing if SgrA* is a WH by observing a hot blob of plasma orbiting near the innermost stable circular orbit (ISCO). Within a few years, NIR observations with GRAVITY will have the capability to directly image hot spots orbiting near the ISCO of SgrA* [21,22] and open a new window to test the actual nature of this object. These data are supposed to come out before the first detection of the shadow. Because of the dramatically different sizes of the photon capture spheres of WHs and BHs, we find that the possible detection of the secondary image of a hot spot orbiting close to the compact object can unambiguously test the possibility that SgrA* is a WH rather than a BH. That will require very good data with a high signal-to-noise ratio, but it is not out of reach. Specific differences may also be present in the hot spot light curve and in the hot spot centroid track, but their features are more model dependent: our hot spot model is too simple to conclude that their observation in real data can distinguish a WH from a BH, and further investigation based on more sophisticated and realistic models would be necessary. With the current results, it seems more likely that light curves and hot spot centroid tracks cannot test the WH scenarios.

II. HOT SPOT MODEL

SgrA* exhibits powerful flares in the x-ray, NIR, and sub-mm bands [23]. During a flare, the flux increases by up to a factor of 10. A flare typically lasts 1–3 hours, and the rate is a few events per day. These flares seem to show a quasiperiodic substructure on a time scale ranging from 13 to about 30 minutes. Several mechanisms have been proposed, such as the heating of electrons in a jet [24], Rossby wave instability in the disk [25], the adiabatic expansion of a blob of plasma [26], and blobs of plasma orbiting at the ISCO of SgrA* [27]. At least some authors have claimed that current observations favor the model of the hot spot near the ISCO [28]. Such a scenario is also supported by some general relativistic magneto-hydrodynamic simulations of accretion flows onto BHs that show that temporary clumps of matter may be common in the region near the

ISCO [29]. Within a few years, the GRAVITY instrument for the ESO Very Large Telescope Interferometer (VLTI) will have the capability to image blobs of plasma orbiting around SgrA* with an angular resolution of about 10 μas and a time resolution of about 1 minute [21,22], and it will thus be possible to test the hot spot model.

For a Kerr BH with a mass $M = 4 \times 10^6 M_\odot$, the ISCO period ranges from about 30 minutes ($a_* = 0$) to 4 minutes ($a_* = 1$ and corotating orbit). The observed period of the quasiperiodic substructure of the flares of SgrA* ranges from 13 to about 30 minutes. If the hot spot model is correct, this means that the radius of the orbit of the hot spot may vary and be larger than that of the ISCO. The shortest period ever measured is 13 ± 2 minutes. If we assume that the latter corresponds to the ISCO period, or at least that it is very close to it, one finds $a_* = 0.70 \pm 0.11$ for $M = 3.6 \times 10^6 M_\odot$ [28]. In Ref. [30], the authors claimed the presence of a quasiperiodic substructure with a period of 5 minutes, which was interpreted as an indication that SgrA* is rotating very fast, with a spin parameter close to 1. However, the analysis of the same data sets in Ref. [31] did not find such a short period substructure.

In the present work, we will consider the simplest hot spot model—that is, a single region of isotropic and monochromatic emission following a geodesic trajectory. Located on the equatorial plane, this hot spot is modeled as an optically thick emitting disk of finite radius. The local specific intensity of the radiation is chosen to have a Gaussian distribution in the local Cartesian space,

$$I_{\rm em}(\nu_{\rm em}, x) \sim \delta(\nu_{\rm em} - \nu_\star) \exp\left[-\frac{|\tilde{\mathbf{x}} - \tilde{\mathbf{x}}_{\rm spot}(t)|^2}{2R_{\rm spot}^2}\right], \quad (1)$$

where $\nu_{\rm em}$ is the photon frequency measured in the rest frame of the emitter, while $\nu_\star$ is the emission frequency of this monochromatic source. The spatial position 3-vector $\tilde{\mathbf{x}}$ is given in pseudo-Cartesian coordinates. Outside a distance of $4R_{\rm spot}$ from the guiding geodesic trajectory $\tilde{\mathbf{x}}_{\rm spot}$, there is no emission. Plausible values are $R_{\rm spot} = 0.1$–$1.0M$, but it depends on the orbital radius, and it is important to check that no point of the hot spot exceeds the speed of light. The specific intensity of the radiation measured by the distant observer is given by

$$I_{\rm obs}(\nu_{\rm obs}, t_{\rm obs}) = g^3 I_{\rm em}(\nu_{\rm em}, t_{\rm obs}), \quad (2)$$

where g is the redshift factor

$$g = \frac{E_{\rm obs}}{E_{\rm em}} = \frac{\nu_{\rm obs}}{\nu_{\rm em}} = \frac{k_\alpha u^\alpha_{\rm obs}}{k_\beta u^\beta_{\rm em}}, \quad (3)$$

k^α is the 4-momentum of the photon, $u^\alpha_{\rm obs} = (-1, 0, 0, 0)$ is the 4-velocity of the distant observer, and $u^\alpha_{\rm em} = (u^t_{\rm em}, 0, 0, \Omega u^t_{\rm em})$ is the 4-velocity of the emitter. Ω is the Keplerian angular frequency of a test particle at the emission radius $r_{\rm e}$. $I_{\rm obs}(\nu_{\rm obs})/\nu^3_{\rm obs} = I_{\rm em}(\nu_{\rm em})/\nu^3_{\rm em}$ follows from the Liouville theorem. The hot spot emission is assumed to be monochromatic and isotropic, with a Gaussian intensity, as shown in Eq. (1). Using the normalization condition $g_{\mu\nu} u^\mu_{\rm em} u^\nu_{\rm em} = -1$, one finds

$$u^t_{\rm em} = -\frac{1}{\sqrt{-g_{tt} - 2g_{t\phi}\Omega - g_{\phi\phi}\Omega^2}}, \quad (4)$$

and therefore,

$$g = \frac{\sqrt{-g_{tt} - 2g_{t\phi}\Omega - g_{\phi\phi}\Omega^2}}{1 + \lambda\Omega}, \quad (5)$$

where $\lambda = k_\phi / k_t$ is a constant of the motion along the photon path. Doppler boosting and gravitational redshift are entirely encoded in the redshift factor g. The effect of light bending is included by the ray-tracing calculation.

The observer's sky is divided into a number of small elements, and the ray-tracing procedure provides the observed time-dependent flux density from each element. By integrating the observed specific intensity over the solid angle subtended by the image of the hot spot on the observer's sky, we obtain the observed flux

$$F(\nu_{\rm obs}, t_{\rm obs}) = \int I_{\rm obs}(\nu_{\rm obs}, t_{\rm obs}) {\rm d}\Omega_{\rm obs} = \int g^3 I_{\rm em}(\nu_{\rm em}, t_{\rm obs}) {\rm d}\Omega_{\rm obs}. \quad (6)$$

If we integrate over the frequency range of the radiation, we get the observed luminosity, or light curve, of the hot spot,

$$L(t_{\rm obs}) = \int F(\nu_{\rm obs}, t_{\rm obs}) {\rm d}\nu_{\rm obs}. \quad (7)$$

A more detailed description of the calculation procedure can be found, for instance, in Ref. [32]. In the present paper, we normalize the light curves by dividing the observed luminosity $L(t_{\rm obs})$ by the corresponding maximum, since only the shape of the light curve can be used to determine the parameters of the model. Such a time-dependent emission signal can be added to a background intensity coming from the inner region of the steady-state accretion disk. By definition, the hot spot will have a higher density and/or higher temperature, and thus a higher emissivity, than the background accretion disk, adding a small modulation to the total flux.

III. TESTING THE WORMHOLE SCENARIO

In the calculations of the electromagnetic radiation emitted by a hot spot, the spacetime metric determines the exact photon propagation from the hot spot to the distant observer, the redshift factor g in Eq. (5), and the

value of the ISCO radius. There are many kinds of WHs proposed in the literature, but not all are viable supermassive BH candidates. For instance, some WHs have vanishing or negative effective gravitational mass. In the present work, we adopt the same asymptotically flat, nonrotating, traversable WH solution discussed in Refs. [15,18], whose line element reads [33]

$$ds^2 = e^{2\Phi(r)}dt^2 - \frac{dr^2}{1-\frac{b(r)}{r}} - r^2 d\theta^2 - r^2\sin^2\theta d\phi^2, \quad (8)$$

where $\Phi(r)$ and $b(r)$ are, respectively, the redshift and the shape functions. A common choice is $\Phi(r) = -r_0/r$, where r_0 is the WH throat radius and sets the scales of the system. r_0 is interpreted as the mass of the object in the Newtonian limit, and in what follows, it will be indicated with M, just to use the same notation in the WH and BH cases. The shape function can be assumed to be of the form

$$b(r) = \frac{M^\gamma}{r^{\gamma-1}}, \quad (9)$$

where γ is a constant. In this paper, we consider the case $\gamma = 1$, but the observational signature that distinguishes WHs and BHs is independent of the value of γ.

Let us now compare the features of the electromagnetic radiation emitted by a blob of plasma orbiting around a WH and a BH. Since the hot spot orbital frequency is the simplest parameter to measure, we want to compare the following three cases:

(1) A hot spot orbiting the traversable WH in Eq. (8) at some radius $r_{\rm WH}$. We indicate its angular frequency with $\Omega_{\rm WH}$.
(2) A hot spot orbiting at the ISCO radius of a Kerr BH with spin parameter such that its Keplerian orbital frequency is $\Omega_{\rm ISCO} = \Omega_{\rm WH}$.
(3) A hot spot orbiting a Kerr BH with spin parameter $a_* = 0.99$ at the equatorial circular orbit with radius $r_{\rm BH}$, whose Keplerian orbital frequency is $\Omega_{\rm BH} = \Omega_{\rm ISCO} = \Omega_{\rm WH}$.

Figure 1 shows the light curves (total and primary image light curves, using blue solid and red dashed lines, respectively) of hot spots orbiting a WH (top panels), a Kerr BH at the ISCO radius (central panels), and a Kerr BH with spin parameter $a_* = 0.99$ (bottom panels). The left panels correspond to hot spots with an angular frequency equal to that of a hot spot around a WH at the ISCO radius, $r_{\rm WH} = 2M$. The right panels correspond instead to hot spots with an angular frequency equal to that of a hot spot around a WH at the radius $r_{\rm WH} = 3M$. One should thus compare the light curves in the same column. The top panels are for the WH case with $r_{\rm WH} = 2M$ (left panel) and $3M$ (right panel). The central panels show the light curves of a hot spot at the ISCO of a Kerr BH, whose spin parameter is $a_* = 0.883911$ (left panel) and 0.673917 (right panel). In the bottom panels, there are the hot spot light curves around a Kerr BH with $a_* = 0.99$: the hot spot orbital radius is $r_{\rm BH} = 2.3807M$ (left panel) and $3.3973M$ (right panel).

The most important difference between the WH and BH cases is that in the BH light curves, there is a small bump marking the maximum intensity of the secondary image light curve, which is instead absent in the WH light curve. The effect is more pronounced when the hot spot is closer to the compact object and tends to disappear as the hot spot radius/frequency increases. While such a feature in the hot spot light curve could potentially represent an observational signature to distinguish WHs and BHs, the actual properties of the bump due to the secondary image depend on the hot spot model (hot spot size, emissivity function, etc.). In Fig. 1, we have considered a single hot spot disk with radius $R_{\rm spot} = 0.15M$ and isotropic and monochromatic emission. The strong gravitational force near the compact object typically tends to destroy the hot spot, which is smeared along its orbit with the result to make the peaks of the images less well defined. Moreover, the substantial background may hide the small bump due to the secondary image in the BH light curves. While a final answer would require a more detailed discussion based on a more realistic model, from these results it seems unlikely that the observation of the light curve of a hot spot can be used to distinguish BHs and WHs, even considering that real data are usually noisy and incomplete.

NIR observations may soon be able to directly image hot spots around SgrA*. For instance, the VLTI instrument GRAVITY is supposed to be operative within a few years and be able of astrometric measurements with an angular accuracy of about 10 μarcsec and a time resolution around 1 minute. Such a values have to be compared with the apparent gravitational radius of SgrA*, M, which is about 5 μarcsec for an object with a mass of 4 million Solar masses and a distance of 8 kpc from us, and with the hot spot orbital period, for which current data point out a time scale in the range 13 to 30 minutes (presumably due to the different orbital radius in different observations). Snapshots of the direct image of hot spots orbiting WHs and BHs are shown in Figs. 2 and 3. Every figure compares the three situations mentioned above, where the images of the hot spot around a WH are in the left column, the ones of a hot spot around a Kerr BH at the ISCO radius are in the central column, while the right column is for the images of a hot spot around a Kerr BH with spin parameter $a_* = 0.99$. Fig. 2 shows the cases in which the hot spot orbiting around the WH has orbital radius $r_{\rm WH} = 2M$, while Fig. 3 is for the WH hot spot with orbital radius $r_{\rm WH} = 3M$. We have thus the two scenarios already discussed in Fig. 1, and therefore the BH parameters are the same.

In all these snapshots, the secondary image is dimmer (in some snapshots almost absent) and smeared along/near the apparent photon capture radius. The apparent photon

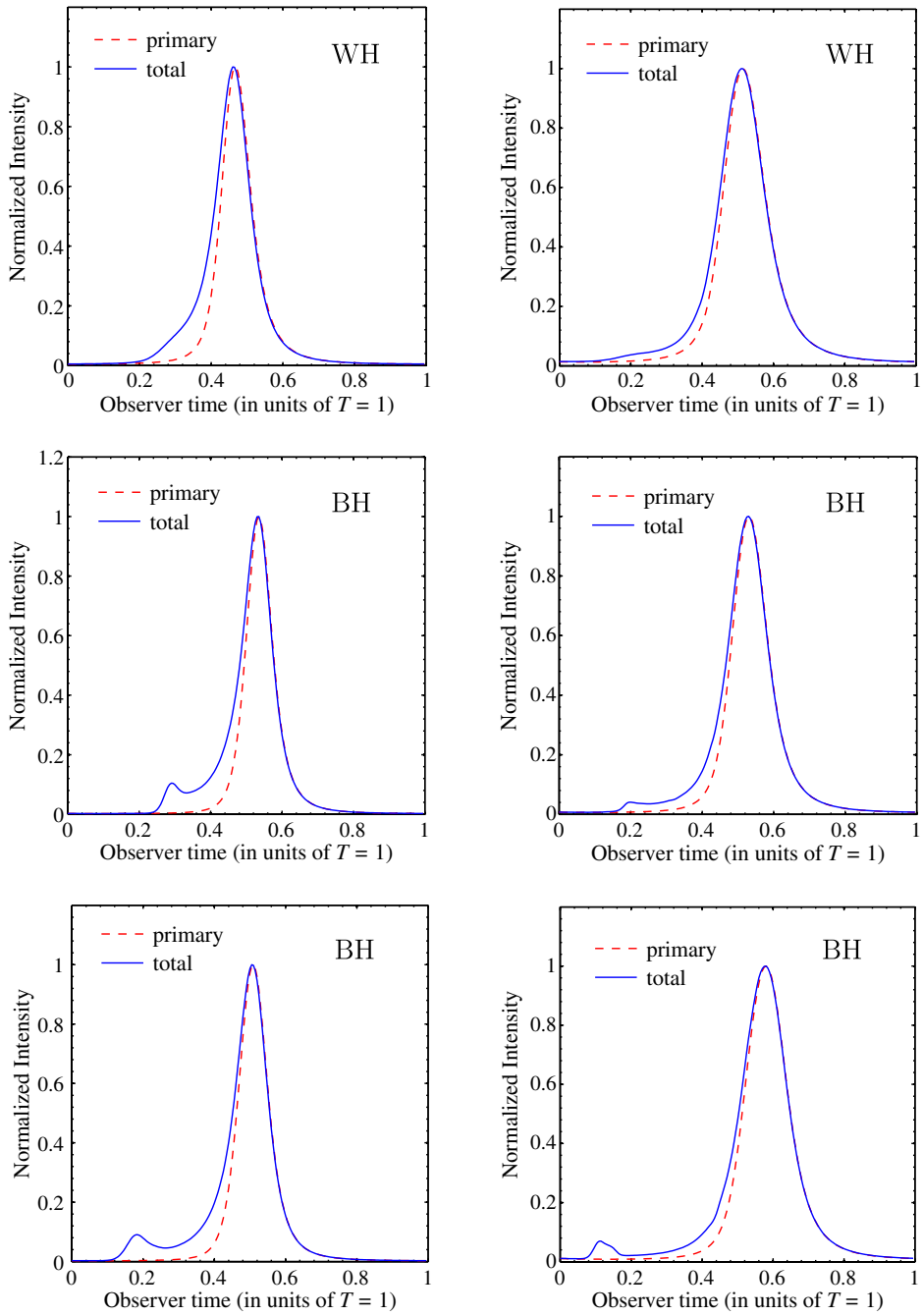

FIG. 1 (color online). Top panels: Total light curves and primary image light curves of a hot spot orbiting around a WH at the ISCO $r_{\rm WH} = 2M$ (left panel) and at the radius $r_{\rm WH} = 3M$ (right panel). The viewing angle of the observer is $i = 60°$, and the hot spot size is $R_{\rm spot} = 0.15M$. Central panels: As in the top panels, for a hot spot orbiting the ISCO of a Kerr BH with spin parameter $a_* = 0.883911$ (left panel) and $a_* = 0.673917$ (right panel); the value of the spin has been chosen to have an orbital frequency equal, respectively, to that of a hot spot orbiting a WH at the ISCO and at the radius $r_{\rm WH} = 3M$. Bottom panels: As in the top and central panels, for a hot spot orbiting a Kerr BH with spin parameter $a_* = 0.99$ at the radius with the same Keplerian orbital frequency as that of a hot spot orbiting a WH at the ISCO (left panel) and at the radius $r_{\rm WH} = 3M$ (right panel). See the text for more details.

capture radius, i.e., the one seen by a distant observer, was computed in Ref. [18] in the case of the WH in Eq. (8), and it turns out to be about $2.718M$. The angular size of the WH on the sky would be about 30 μarcsec for SgrA*. In the case of a Kerr BH, the apparent photon capture radius is about twice that, with a small dependence on the BH spin and observer's inclination angle. For SgrA*, it would be around 50 μarcsec. In particular, the top panels in Figs. 2 and 3 clearly show the difference between the hot spot secondary images in the cases of WHs and BHs.

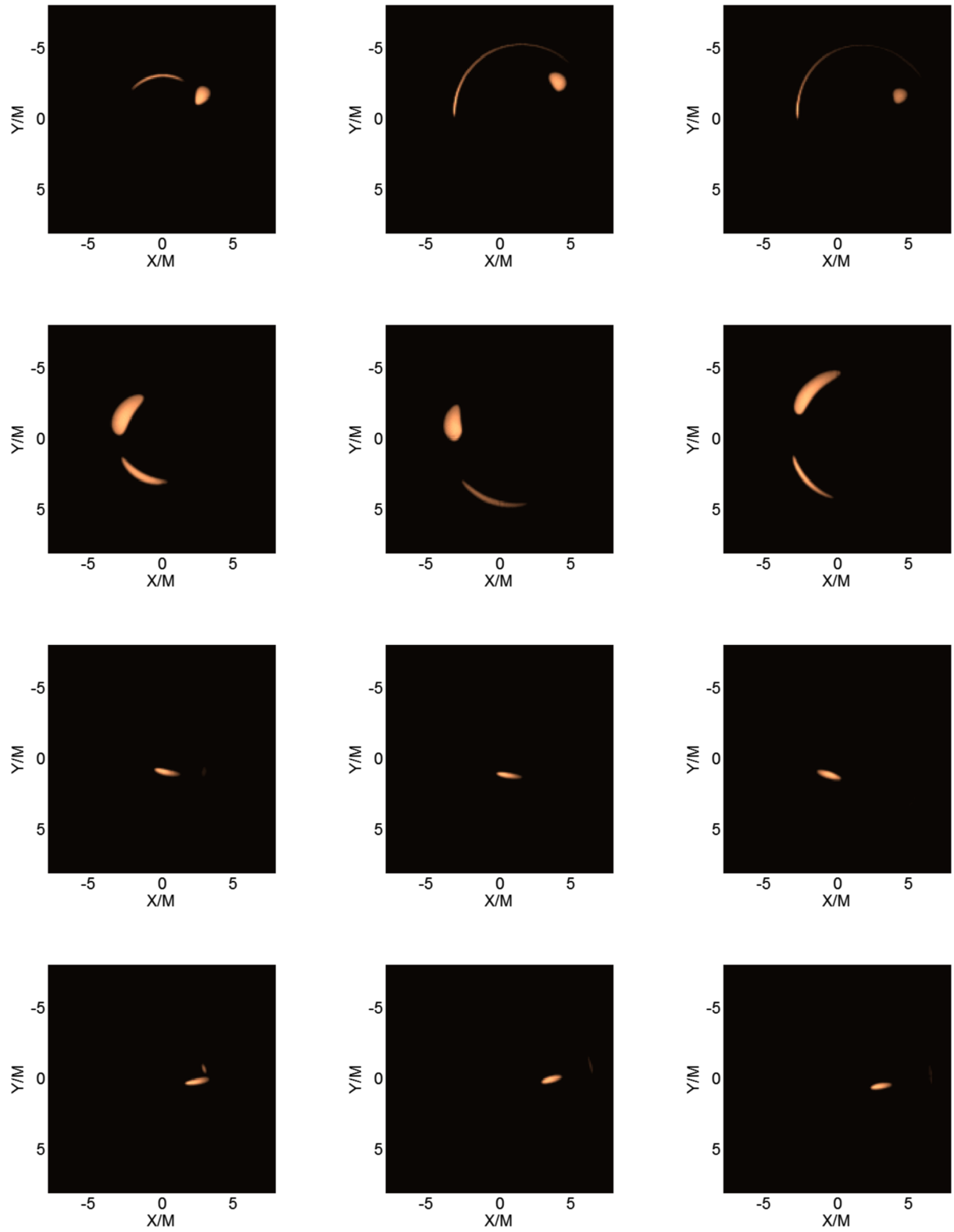

FIG. 2 (color online). Left panels: Snapshots of a hot spot orbiting a WH at the ISCO. Central panels: Snapshots of a hot spot orbiting a Kerr BH with spin parameter $a_* = 0.883911$ at the ISCO; the value of the spin parameter has been chosen to have the same orbital frequency as that of the hot spot orbiting the ISCO of the WH. Right panel: Snapshots of a hot spot orbiting a Kerr BH with spin parameter $a_* = 0.99$ at the radius with Keplerian orbital frequency equal to the frequency of the hot spots of the other two cases. The time interval between two adjacent panels in the same column is $T/4$, where T is the hot spot orbital period. In all these simulations, the inclination angle of the hot spot orbital plane with respect to the line of sight of the observer is $i = 60°$, and the hot spot radius is $R_{\rm spot} = 0.15M$. See the text for more details.

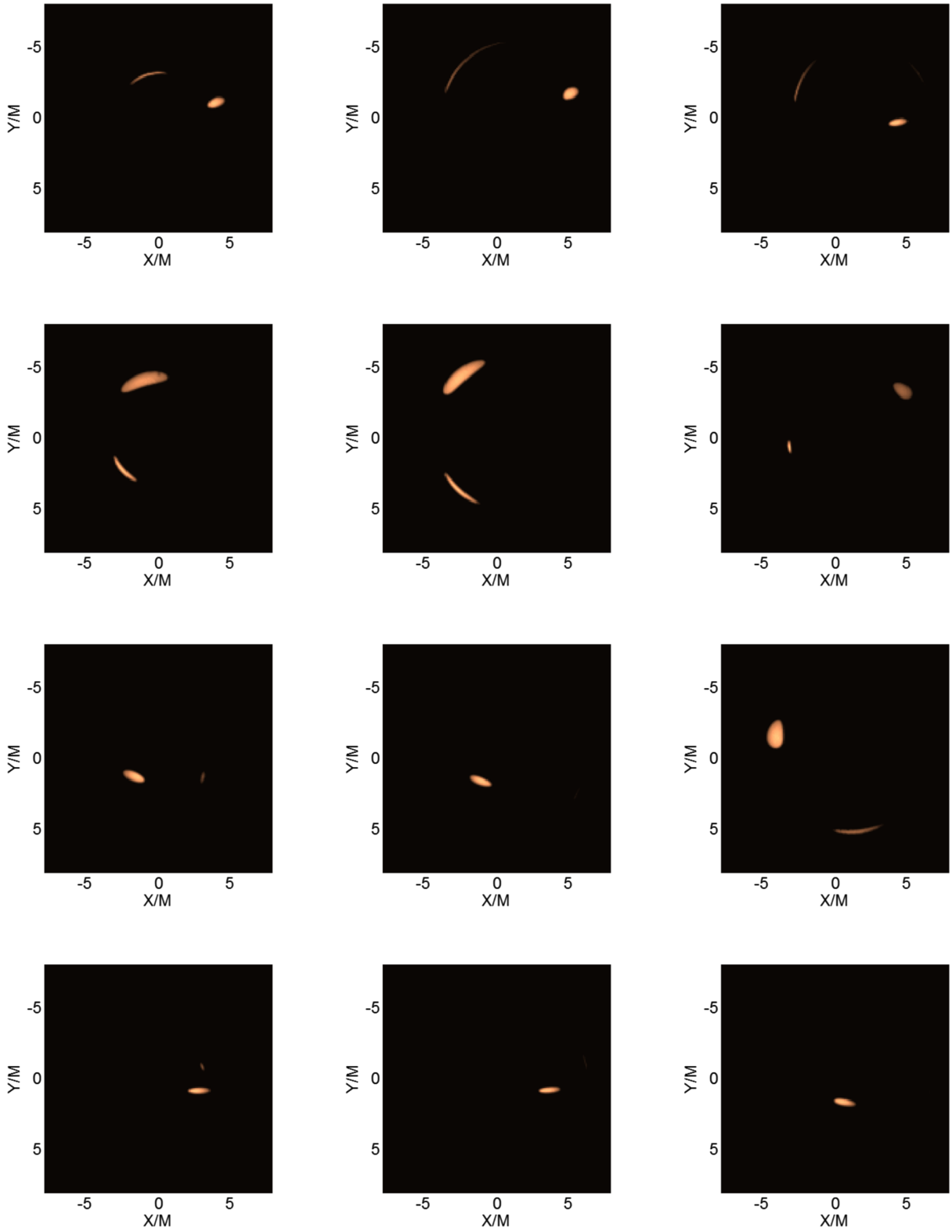

FIG. 3 (color online). As in Fig. 2, for a hot spot orbiting a WH at the radius $r_{\rm WH} = 3M$ (left panels), a Kerr BH with spin parameter $a_* = 0.673917$ at the ISCO (central panels; the value of the spin parameter has been chosen to have the same hot spot orbital period as the one around the WH), and a Kerr BH with spin parameter $a_* = 0.99$ and at the radius with Keplerian orbital period equal to that of the other two cases (right panels). See the text for more details.

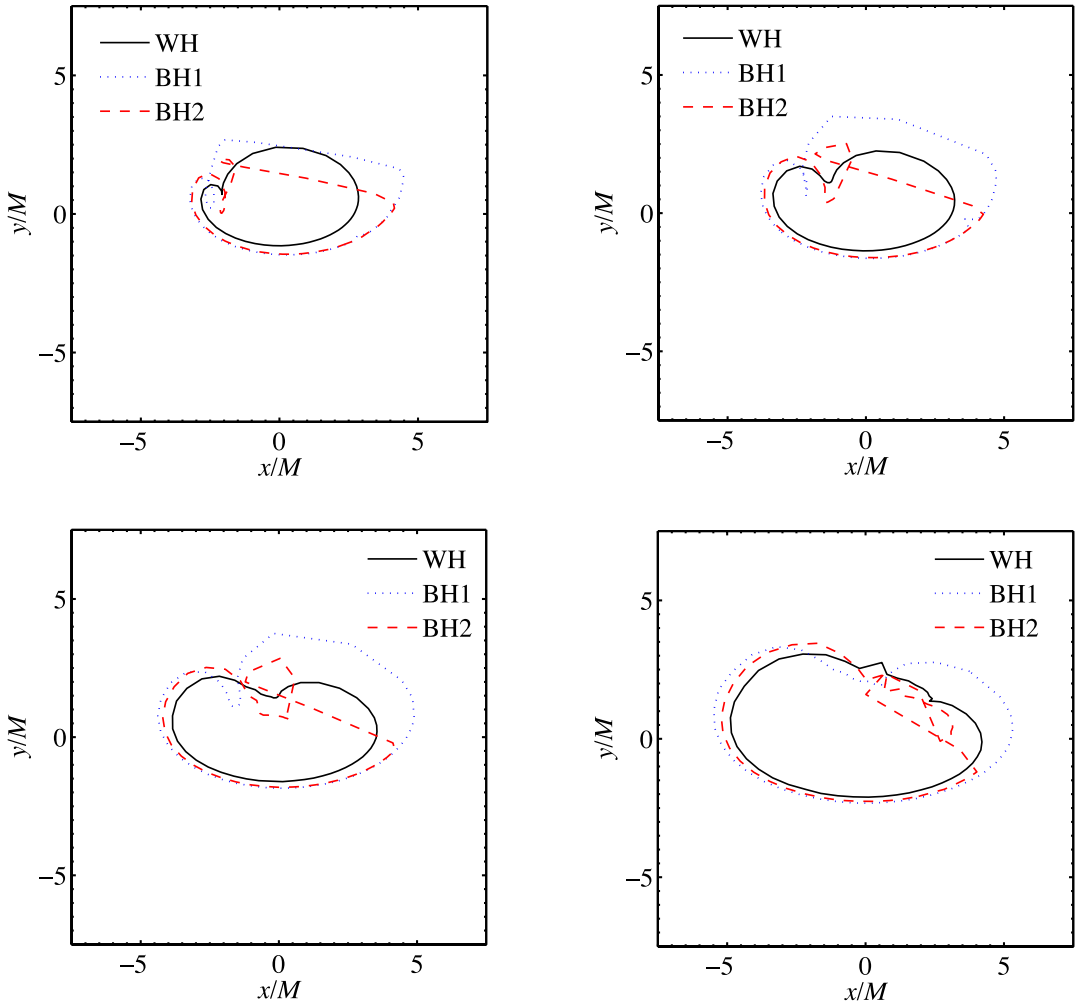

FIG. 4 (color online). Centroid tracks of a hot spot orbiting a WH (black solid curves), a BH at the ISCO radius with spin parameter such that the hot spot orbital frequency is the same as that around the WH (blue dotted curves), and a BH with spin parameter $a_* = 0.99$ and at the radius with the same Keplerian orbital frequency as one of the hot spots in the other two cases (red dashed curves). The orbital radius of the hot spot around the WH is $r_{\rm WH} = 2M$ (ISCO radius; top-left panel), $r_{\rm WH} = 2.5M$ (top-right panel), $r_{\rm WH} = 3M$ (bottom-left panel), and $r_{\rm WH} = 4M$ (bottom-right panel). The inclination angle of the hot spot orbital plane with respect to the observer is $i = 60°$, and the hot spot size is $R_{\rm spot} = 0.15M$. See the text for more details.

The primary images are fairly similar, while the secondary images are smeared along the apparent photon sphere, which is much smaller in the WH case. Let us also notice that such a prediction does not depend on the hot spot model (hot spot size, spectrum, observer's viewing angle, etc.), but only on the spacetime metric around the compact object. While observationally challenging, the detection of the hot spot secondary image and the estimate of the apparent photon capture radius are not out of reach in the near future, and they seem to be the observational signature to distinguish WHs and BHs. Let us also note that the apparent photon capture radius depends only on the redshift function $\Phi(r)$, while it is independent of the shape function $b(r)$ [18].

Lastly, we have computed the hot spot centroid tracks. Figure 4 shows four examples with different hot spot orbital periods. The left panels show the two cases discussed in Figs. 1–3, in which the hot spot around the WH has the orbital radius $r_{\rm WH} = 2M$ (top-left panel in Fig. 4) and $r_{\rm WH} = 3M$ (bottom-left panel in Fig. 4). In the top-right panel in Fig. 4, the hot spot around the WH has the orbital radius $r_{\rm WH} = 2.5M$, while in the bottom-right panel the orbital radius is $r_{\rm WH} = 4M$. In Fig. 4, the hot spot size is $R_{\rm spot} = 0.15M$, and the observer's viewing angle is still $i = 60°$. While one may be tempted to argue that the centroid tracks of WHs and BHs present different features, and therefore that its detection can distinguish WHs and BHs, as discussed in Ref. [27], the exact hot spot model is quite important. Since we are considering here a very simple model, it is not possible to figure out if the detection of the centroid track can be used to distinguish WHs and BHs. From the simple model considered here, the difference between WHs and BHs does not seem to be so clear and easy to identify.

IV. SUMMARY AND CONCLUSIONS

WHs are topologically nontrivial structures connecting either two different regions of our Universe or two different universes in a multiverse model. While of exotic nature, they are allowed in general relativity and in alternative theories of gravity, and they are viable candidates to explain the supermassive objects harbored at the center of every normal galaxy. In the present paper, we have extended the studies of Refs. [15,18], and we have further investigated if observations can test the possibility that the supermassive BH candidates in galactic nuclei are instead WHs. We have focused our attention on the specific case of the metric in Eq. (8), which describes an asymptotically flat, nonrotating, traversable WH. In Ref. [15], it was found that such a WH would be consistent with current observations of the iron Kα line detected in the x-ray spectrum of supermassive BH candidates. In Ref. [18], it was pointed out that the observation of the shadow of SgrA*, the supermassive BH candidate at the center of the Milky Way, could easily test the possibility that this object is actually a WH rather than a BH, because the size of the shadow, which corresponds to the apparent photon capture sphere, is much smaller in the WH case than in the BH one.

In this paper, we have discussed the possibility of testing the presence of a WH at the center of our Galaxy by observing a hot blob of plasma orbiting near the ISCO of SgrA*. Such of observations are expected to be possible soon in the NIR, before the first detection of the shadow of SgrA*, thanks to the advent of the VLTI instrument GRAVITY. We have found that the features of the hot spot secondary image are substantially different between a WH and a BH, and they probably represent the key point at which to distinguish the two scenarios. If the hot spot is close to the compact object, even if it is not necessarily at the ISCO radius, the secondary image shows up around the apparent photon capture sphere, which is significantly different in the two spacetimes. The size of the WH photon capture radius projected on the observer sky is indeed about half the BH one, and in the case of SgrA* they correspond, respectively, to about 30 and 50 μarcsec. The detection of the direct image of the secondary image of a hot spot could thus test if SgrA* is a WH rather than a BH. Such a prediction is very general, in the sense that it does not depend on the hot spot model and on the inclination angle of the hot spot orbital plane with respect to the line of sight of the observer. The apparent photon capture radius only depends on the spacetime geometry close to the compact object. Specific features of the secondary image are also encoded in the hot spot light curve and in its centroid track. However, these features do depend on the hot spot model, and within our simple setup it is not possible to figure out if future observations of light curves and centroid tracks can distinguish WHs and BHs.

A small apparent radius of the photon capture sphere, which is here the true observational signature to distinguish WHs from BHs, can be found even in other contexts. Generally speaking, a similar property can be expected in the case of naked singularities, which have also been considered as possible candidates to explain the supermassive objects at the centers of galaxies. The absence of an event horizon is an indication of the fact that the gravitational field around them is weaker than the one around a BH and, at least in some cases studied in the literature, the photon capture sphere of these objects is indeed very small [34]. However, these spacetimes may be unstable. This is, for example, the case of the Kerr spacetime with $a > M$: the existence of an ergoregion and the absence of event horizons make the spacetime very unstable, and therefore these objects cannot be considered as serious candidates [35].

Lastly, one may wonder whether the recently announced cloud close to SgrA* and supposed to be soon swallowed by the central supermassive objects may be a unique opportunity to test the actual nature of SgrA* [36] and the possible observational predictions in the case of a BH and of a WH. Actually, it seems now that the accretion process onto the central object will be much slower than what it was initially supposed (just because the gas takes time to lose energy and angular momentum), and therefore it is now thought that there will be no violent event, and the time scale will be so long that the difference in the accretion rate onto SgrA* will probably be irrelevant.

ACKNOWLEDGMENTS

This work was supported by NSFC Grant No. 11305038, the Shanghai Municipal Education Commission Grant for Innovative Programs No. 14ZZ001, the Thousand Young Talents Program, and Fudan University.

[1] M. Visser, Phys. Rev. D **39**, 3182 (1989); **41**, 1116 (1990).
[2] H. Kodama, M. Sasaki, K. Sato, and K.-i. Maeda, Prog. Theor. Phys. **66**, 2052 (1981); D. Garfinkle and A. Strominger, Phys. Lett. B **256**, 146 (1991).
[3] J. Kormendy and D. Richstone, Annu. Rev. Astron. Astrophys. **33**, 581 (1995).
[4] S. Gillessen, F. Eisenhauer, S. Trippe, T. Alexander, R. Genzel, F. Martins, and T. Ott, Astrophys. J. **692**, 1075 (2009).

[5] A. M. Ghez, S. Salim, S. D. Hornstein, A. Tanner, M. Morris, E. E. Becklin, and G. Duchene, Astrophys. J. **620**, 744 (2005).
[6] E. Maoz, Astrophys. J. **494**, L181 (1998).
[7] A. E. Broderick, A. Loeb, and R. Narayan, Astrophys. J. **701**, 1357 (2009).
[8] C. Bambi, Phys. Rev. D **83**, 103003 (2011); **85**, 043001 (2012); Phys. Lett. B **705**, 5 (2011); Phys. Rev. D **87**, 023007 (2013).
[9] C. Bambi, Mod. Phys. Lett. A **26**, 2453 (2011); Astronomy Review **8**, 4 (2013).
[10] X. Fan *et al.* (SDSS Collaboration), Astron. J. **122**, 2833 (2001); D. J. Mortlock *et al.*, Nature (London) **474**, 616 (2011).
[11] M. Volonteri and J. Bellovary, Rep. Prog. Phys. **75**, 124901 (2012).
[12] A. Dolgov and J. Silk, Phys. Rev. D **47**, 4244 (1993).
[13] L. C. Ho, arXiv:astro-ph/0401526; J. Kormendy and L. C. Ho, Annu. Rev. Astron. Astrophys. **51**, 511 (2013).
[14] R. D. Blandford and R. L. Znajek, Mon. Not. R. Astron. Soc. **179**, 433 (1977).
[15] C. Bambi, Phys. Rev. D **87**, 084039 (2013).
[16] G. S. Bisnovatyi-Kogan and S. I. Blinnikov, Astron. Astrophys. **59**, 111 (1977); R. D. Blandford and D. G. Payne, Mon. Not. R. Astron. Soc. **199**, 883 (1982); S. Takeuchi, K. Ohsuga, and S. Mineshige, Publ. Astron. Soc. Jpn. **62**, L43 (2010); X. Cao, Astrophys. J. **783**, 51 (2014).
[17] R. Fender, E. Gallo, and D. Russell, Mon. Not. R. Astron. Soc. **406**, 1425 (2010); D. M. Russell, E. Gallo, and R. P. Fender, Mon. Not. R. Astron. Soc. **431**, 405 (2013); R. Narayan and J. E. McClintock, Mon. Not. R. Astron. Soc. **419**, L69 (2012); J. F. Steiner, J. E. McClintock, and R. Narayan, Astrophys. J. **762**, 104 (2013).
[18] C. Bambi, Phys. Rev. D **87**, 107501 (2013).
[19] H. Falcke, F. Melia, and E. Agol, Astrophys. J. **528**, L13 (2000).
[20] C. Bambi and N. Yoshida, Classical Quantum Gravity **27**, 205006 (2010); C. Bambi, F. Caravelli, and L. Modesto, Phys. Lett. B **711**, 10 (2012); Z. Li and C. Bambi, J. Cosmol. Astropart. Phys. 01 (2014) 041; N. Tsukamoto, Z. Li, and C. Bambi, J. Cosmol. Astropart. Phys. 06 (2014) 043.
[21] F. Eisenhauer *et al.*, Messenger **143**, 16 (2011); F. H. Vincent, T. Paumard, G. Perrin, L. Mugnier, F. Eisenhauer, and S. Gillessen, Mon. Not. R. Astron. Soc. **412**, 2653 (2011).
[22] http://www.mpe.mpg.de/ir/gravity.
[23] R. Genzel, R. Schödel, T. Ott, A. Eckart, T. Alexander, F. Lacombe, D. Rouan, and B. Aschenbach, Nature (London) **425**, 934 (2003); A. M. Ghez, S. A. Wright, K. Matthews, D. Thompson, D. Le Mignant, A. Tanner, S. D. Hornstein, M. Morris, E. E. Becklin, and B. T. Soifer, Astrophys. J. **601**, L159 (2004); A. Eckart *et al.*, Astron. Astrophys. **427**, 1 (2004); K. Dodds-Eden *et al.*, Astrophys. J. **728**, 37 (2011); G. Trap *et al.*, Astron. Astrophys. **528**, A140 (2011).
[24] S. Markoff, H. Falcke, F. Yuan, and P. L. Biermann, Astron. Astrophys. **379**, L13 (2001).
[25] M. Tagger and F. Melia, Astrophys. J. **636**, L33 (2006).
[26] F. Yusef-Zadeh, D. Roberts, M. Wardle, C. O. Heinke, and G. C. Bower, Astrophys. J. **650**, 189 (2006).
[27] N. Hamaus, T. Paumard, T. Müller, S. Gillessen, F. Eisenhauer, S. Trippe, and R. Genzel, Astrophys. J. **692**, 902 (2009).
[28] S. Trippe, T. Paumard, T. Ott, S. Gillessen, F. Eisenhauer, F. Martins, and R. Genzel, Mon. Not. R. Astron. Soc. **375**, 764 (2007).
[29] J.-P. De Villiers, J. F. Hawley, and J. H. Krolik, Astrophys. J. **599**, 1238 (2003); J. D. Schnittman, J. H. Krolik, and J. F. Hawley, Astrophys. J. **651**, 1031 (2006).
[30] B. Aschenbach, N. Grosso, D. Porquet, and P. Predehl, Astron. Astrophys. **417**, 71 (2004).
[31] G. Belanger, R. Terrier, O. C. De Jager, A. Goldwurm, and F. Melia, J. Phys. Conf. Ser. **54**, 420 (2006).
[32] Z. Li, L. Kong, and C. Bambi, Astrophys. J. **787**, 152 (2014).
[33] T. Harko, Z. Kovacs, and F. S. N. Lobo, Phys. Rev. D **78**, 084005 (2008).
[34] C. Bambi and K. Freese, Phys. Rev. D **79**, 043002 (2009).
[35] G. Dotti, R. J. Gleiser, I. F. Ranea-Sandoval, and H. Vucetich, Classical Quantum Gravity **25**, 245012 (2008); P. Pani, E. Barausse, E. Berti, and V. Cardoso, Phys. Rev. D **82**, 044009 (2010).
[36] S. Gillessen, R. Genzel, T. K. Fritz, E. Quataert, C. Alig, A. Burkert, J. Cuadra, F. Eisenhauer *et al.*, Nature (London) **481**, 51 (2012).